

Heavy Flavour Tagging in CDF

A. Menzione

INFN, Pisa

1. Introduction

This contribution is focused on the physical importance of secondary vertices recognition in the search for rare events with heavy flavour content.

A description of the system foreseen for CDF and an outline of its features are given in the following. In particular, we discuss the improvements in a number of quality factors of the detector, other than vertex tagging, which are obtained through the implementation of the vertex detector.

Based on detailed simulations, examples are given which illustrate the effectiveness of the system to reject background from light quark events. Efficiencies expected for a number of channels of physical importance are quoted.

2. Relevance of the heavy flavour tag

The search for secondary vertices is an alternative and complementary approach to heavy flavour physics with respect to more traditional weapons like missing E_t or large p_t leptons. Since technology now allows to build an adequate system for 2000 GeV $p\bar{p}$ collisions, we believe that the chance should be exploited. One would thus enable CDF to cover exciting fields of research. One way for instance would be to tag hadronic decays of heavy flavours. In the heavy quark decay chain, b-quarks and to a lesser extent c-quarks may be detected exploiting the finite lifetime of the heavy flavoured hadrons. This approach would not only be powerful in the search for a fourth generation of quarks, but also can be decisive in a search for other new heavy particles having large decay widths into heavy flavours (e.g. Higgs)⁽¹⁾.

The detection of secondary vertices sorts out at the same time the tracks coming from them, thus reducing greatly the combinatorial background. In a number of cases it might become possible to reconstruct the final state heavy flavoured hadrons.

Fig. 1 gives at the parton level the semileptonic decay chain of a $b\bar{b}$ pair. Also in these next-to-dominant channels hadronization would provide the possibility of observing secondary vertices and then determine which lepton corresponds to which decay. While trying to isolate hard scattering of partons into heavy quark pairs the background would mainly be due to

production of soft pairs of heavy flavours in the same jet (see figures 2a and 2b). UA1 finds that c-production in a specific channel⁽²⁾ is consistent with a large overall yield of charmed hadrons. Fig.3 shows that the two mechanisms can give comparable yields over a large range of p_t ⁽³⁾. It is hoped that accurate tracking may disentangle these two categories by means of the different space distribution of decay vertices and of the different momentum of the heavy flavours relative to the jet.

3. The detector

Finding secondary vertices means an accurate tracking near the interaction point. The goal is to reconstruct the impact parameter of each track with $p_t \gtrsim \langle p_t \rangle$ with an accuracy of $\sim 20 \mu\text{m}$ over a wide rapidity range (± 2 units). The granularity of the system, which determines the pattern recognition capability in intrigued high multiplicity events, should be large. On the other hand, it is realistic to require that the number of additional tracking channels concentrated in a small volume as near as possible to the beam pipe (2" diameter in the CDF case) should not be larger than the corresponding number of the main central tracking system of CDF.

An approach that meets approximately the above two requirements is to use arrays of multielectrode silicon detectors. In fig.4 the location and the dimensions of the system relative to the overall CDF detector are indicated. Fig.5 gives an artist exploded view of part of the apparatus. The entire system will be ~ 60 cm long in order to have good pseudorapidity coverage even accounting for the non negligible length of the interaction region ($\sim \pm 20$ cm). There are four polygonal layers of rectangular crystals. An ultimate goal is to use $50 \mu\text{m}$ pitch electrodes, parallel to the beam line. Table 1 gives a summary of the geometrical characteristics. This system, which is now under study, would be a significant upgrade of the detector that was originally designed and is being prototyped at present⁽⁴⁾. We are planning to use at both ends of the detector a readout system based upon a new monolithic 128-channels preamp and multiplexer⁽⁵⁾ called Microplex, that fits the $50 \mu\text{m}$ pitch and reduces dramatically the number of readout cables. Relevant parameters of the system are summarized in table 2.

4. Improvement of CDF performances

The Silicon Vertex Detector (SVX) provides further information to be combined with the information provided by the main tracking system of CDF, the central Tracking Chamber (CTC) and by the Vertex Time Projection Chambers (VTPC's) (see fig.4). First of all, four additional points far away from the CTC are measured with high accuracy. This improves the momentum

resolution. In addition, a precise location of the event vertex is provided which might provide a useful constraint in a number of cases.

A study was made⁽⁶⁾ of how much the information from the SVX would be beneficial for CDF. All active and passive material was accounted for. This comparison shows that the introduction of SVX not only improves the impact parameter resolution by a factor of 5 (the goal for which SVX is designed for), but also the error in momentum measurement is reduced by a factor of two and the error in φ_0 (azimuthal angle at the origin) is reduced by a factor of three.

Fig.6 illustrates, as a function of p_t , the behaviour of these errors when the various devices are activated. It might be noticed (fig.6a) that almost no help in momentum measurement comes from the SVX for secondaries of $p_t \lesssim 3$ GeV. A reduction of the pipe diameter would help in getting a better momentum resolution, as well as a smaller error in the impact parameter as shown in fig.7.

5. The method for finding secondary vertices

The minimum signature of a secondary vertex is a track not coming from the main event vertex. In practice to localize a secondary vertex well we need at least three tracks. A convenient representation of the event is obtained by making use of the conjugate plane where each track in the real R, φ space is represented by a point⁽⁴⁾. The circular equation of the transverse projection of a track can be written in the form $y=ax+b$. In the conjugate plane a point of coordinates (a,b) represents the track. Tracks originating from the same vertex will be represented in the (a,b) plane by points lying on a straight line. Events with a single main vertex will generate a single straight line. If secondary vertices exist their tracks will be represented by points lying (in general) outside the main vertex line. These points can be associated into different straight lines. If these lines are found, the secondary vertices are found. This method has also the advantage that errors may be propagated in a simple way. A first indication of the existence of secondary vertices can be given by the existence of points outside the main straight line by more than, say, three standard deviations. This flag might be simple enough to be exploited in some higher level trigger implemented in hardware. Fig.8,9 and 10 give (in the order) the distribution of the a-parameter (normalized to its standard error) for tracks of the main vertex, for tracks coming from c decay and for tracks coming from b decay. One sees that the c and b distributions are inconsistent with pure gaussians with $\sigma=1$. In the b-case the large tails at $a/\sigma \gg 1$ indicate the feasibility of tagging secondary vertices.

6. Efficiencies

Fig.11 is the representation in the conjugate plane of a $p\bar{p} \rightarrow b\bar{b}$ event where both decays are correctly found and sorted out. Table 3 gives efficiencies for the charm and beauty channels⁽⁴⁾. The definition of a secondary vertex is three or more aligned tracks out by at least 3 standard deviations from $a=0$. This efficiency has been computed under several hypotheses: first is the case of point-like source and perfect resolution. In this case, only neutral and low multiplicity decay channels and very early decays are not detected. Next the finite size of the source is taken into account (more forward and backward secondaries escape detection). Third, a finite resolution is considered (pattern recognition problems arise and errors in their a -parameter increase). Fourth, an artificial increase of the $R\varphi$ resolution is simulated in order to show how important resolution and granularity are.

It can be seen from fig.10 and from table 3 that the situation is very promising at least for the b case.

We also studied how well the system performs in the challenging task of looking for the decay $W \rightarrow tb$ in the hadronic channels. The lepton signature which provides UA1 with some evidence of the existence of the top is in this case not available. Fig.12 gives the comparison of the signal with the overall QCD background from scattering of light quarks and gluons as well as of heavy quarks. It can be seen in the continuum-subtracted jet-jet mass spectrum of fig.13 that no significant W signal appears after one nominal CDF year ($\int Ldt=10^{36} \text{ cm}^{-2}$). If we apply to the same sample the request of at least one secondary vertex we have (after assuming that non-leading b 's can be rejected by suitable cuts⁽¹⁾) some evidence of a peak at the W mass (fig.14). The different peak significance with and without SVX is also shown in fig.15 that refers to a larger statistics ($\int Ldt=10^{37} \text{ cm}^{-2}$).

The rejection power that one finds with the present SVX design and ISAJET events is summarized in table 4. Even within the present design one sees that while being efficient to $\sim 35\%$ for good $W \rightarrow tb$ events we can reduce the light quarks and gluon background by a factor of $\gtrsim 100$.

7. Conclusion

The use of silicon crystals enables us to realize a detector capable of seeing secondary vertices of particles decaying with lifetimes $\gtrsim 10^{-12}$ sec. The determination of these vertices groups the tracks in bundles thus helping in understanding the decay chain. Overall figures of merit of CDF improve by important factors, e.g. $\Delta p_t/p_t$ improves by a factor two. A search for new rare events in hadron channels may become feasible with the SVX, while being impossible without it.

8. References

- (1) G.Bellettini, "Physics at the Tevatron Collider", Proc. of the Aspen Winter Conference Series, Jan 6th-12th, 1985, INFN/AE-PI1.
G.Chiarelli, "Heavy Flavour Physics with CDF", Pisa University Thesis, INFN/AE-PI2.
- (2) R.Frey, UA1 Collaboration, Proc. of the 4th Topical Workshop on Proton-Antiproton Collider Physics, Bern 1984.
- (3) F.Halzen and F.Herzog, MAD/PH/185, June 1984.
- (4) F.Bedeschi and G.Chiarelli, "Simulation of the Silicon Vertex Detector", CDF 284.
- (5) S.Parker, "A Vertex Detector for e^+e^- Colliders using Silicon Strip Detectors, "Vertex Detectors: Charm and Beauty I", Fermilab Workshop, 21-22 September 1984.
- (6) F.Bedeschi and G.Chiarelli, "Track Impact Parameter and Momentum Resolution combining SVX+VTPC+CTC", CDF 283.

Table 1

Layer	Thickness (μm)	Shape	Internal Diameter (mm)	Length (mm)	Size of crystals (mm^2)	Pitch (μm)	Channels
1	200	Octogonal	30	600	26x75	50	8.032
2	200	"	43	600	36x75	50	11.200
3	200	Dodecagonal	70	600	36x75	100	8.880
4	200	"	80	600	42x75	100	10.200

Table 2

Wafer diameter	4"
Detector thickness	200 μm
Bulk resistivity	3000 \div 5000 $\Omega\cdot\text{cm}$
Bias	Overdepletion
Pitch (inner layer)	50 μm
Space resolution	50 / $\sqrt{72} \approx 15 \mu\text{m}$
Power/channel	5 mW
Signal/noise (m.i.p.)	15/1

Table 3

σ_z (cm)	pitch (μ m)	tagging efficiency for charm (%)	tagging efficiency for beauty (%)
0	0	10	69
0	50	5.5	42
20	50	3.5	36
0	100	2.	25

Table 4

Process	ϵ_3 (%)	ϵ_4 (%)
$W \rightarrow t\bar{b}$	36.5	17.0
$\rightarrow c\bar{s}$	2.0	0.0
$b\bar{b}$	35.3	22.4
$c\bar{c}$	1.6	0.4
u.d.s.g.	0.8	0.4

ϵ_3 = efficiency for finding a vertex containing three tracks

ϵ_4 = efficiency for finding a vertex containing four tracks.

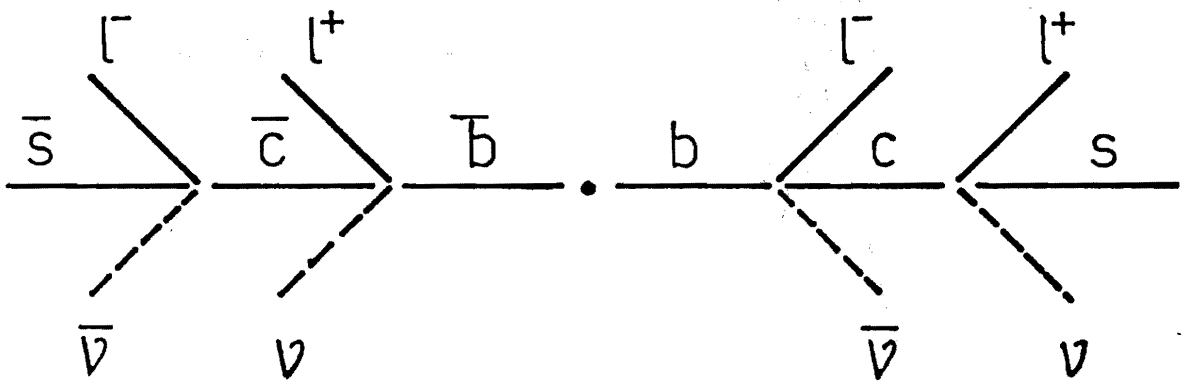


Fig.1

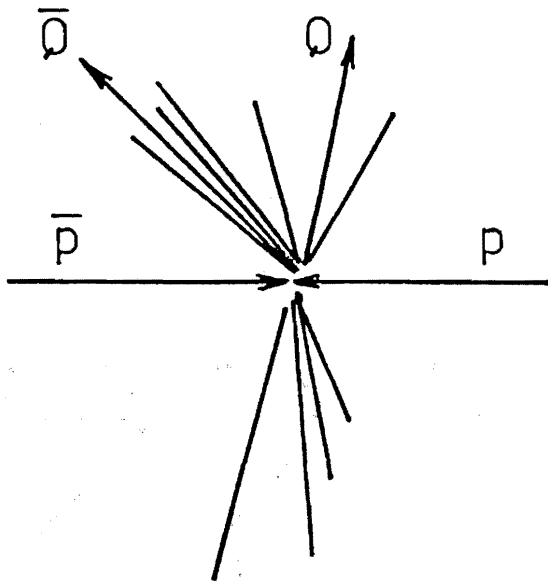


Fig. 2a

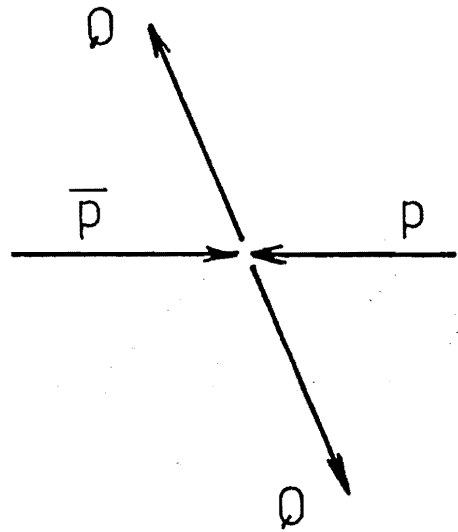


Fig. 2b

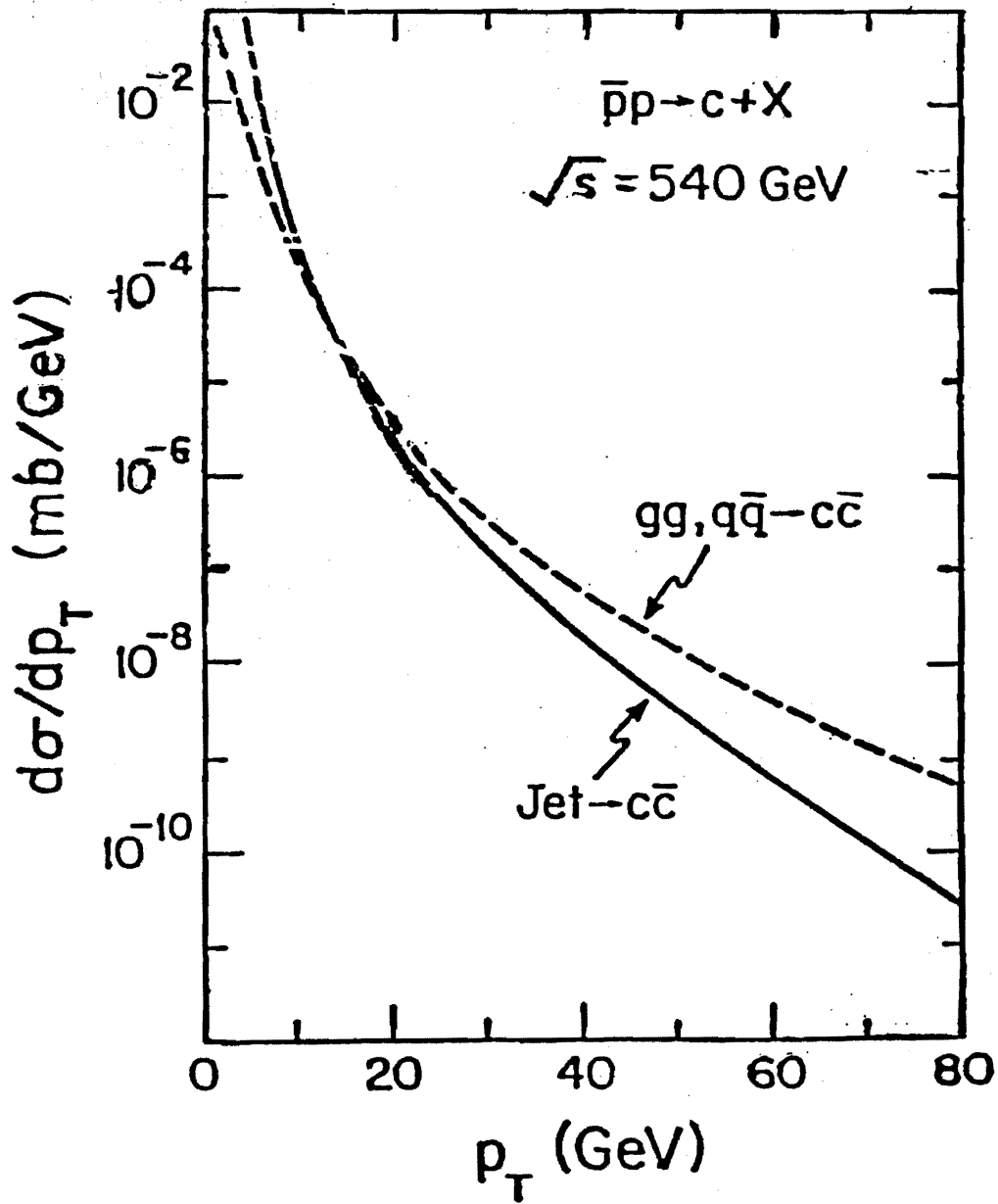


Fig. 3

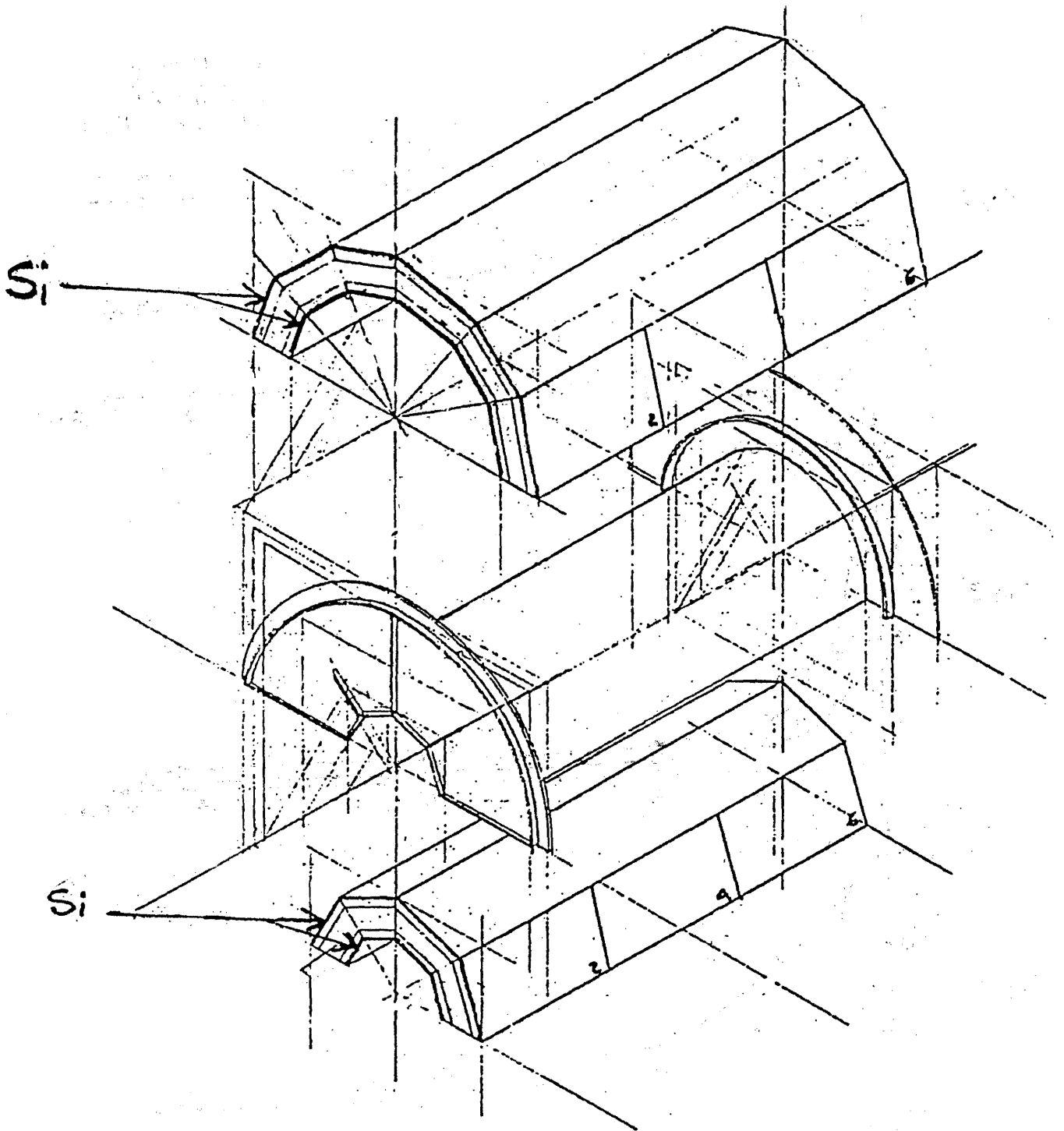


Fig. 5

SVX in

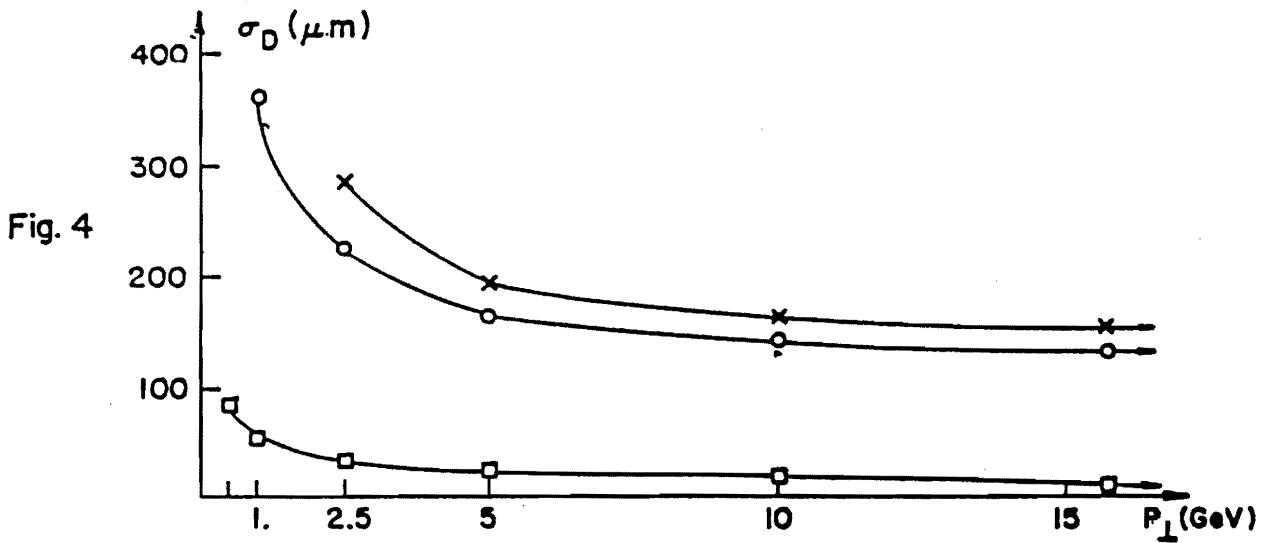
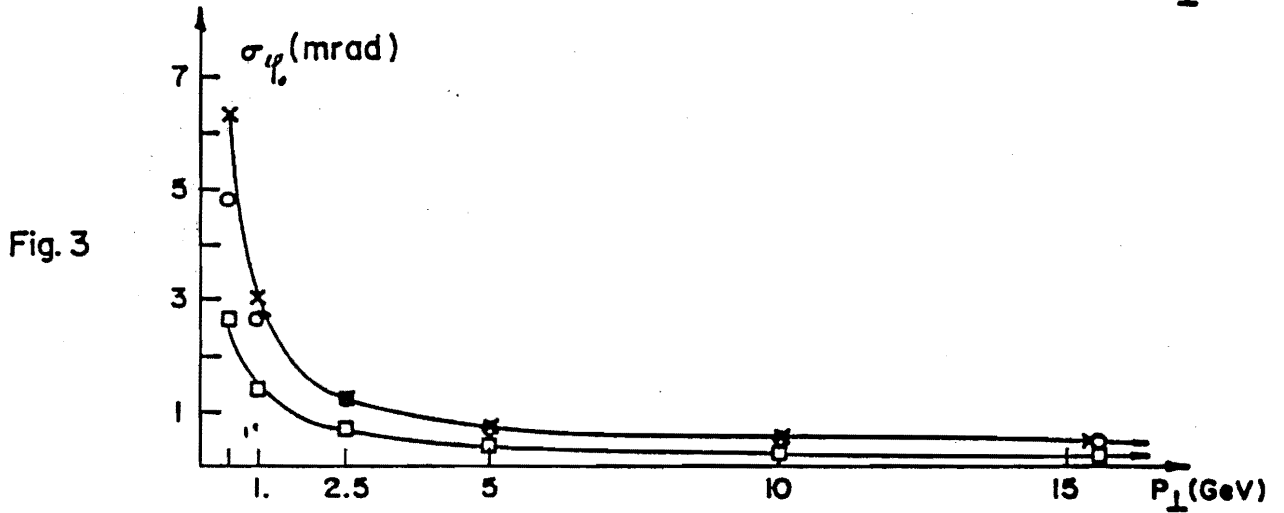
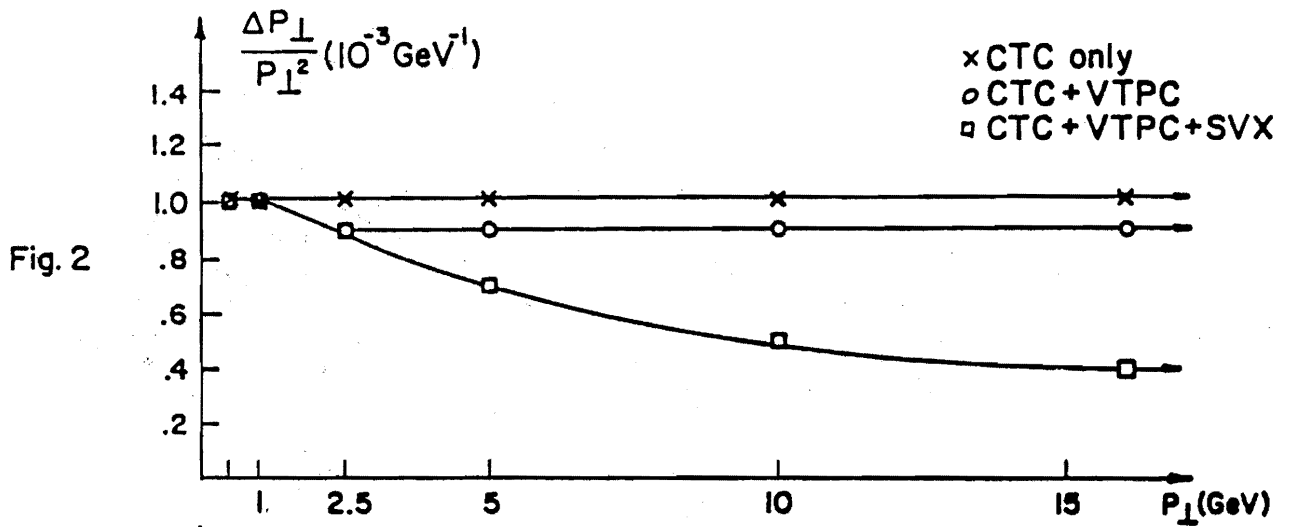


Fig. 6

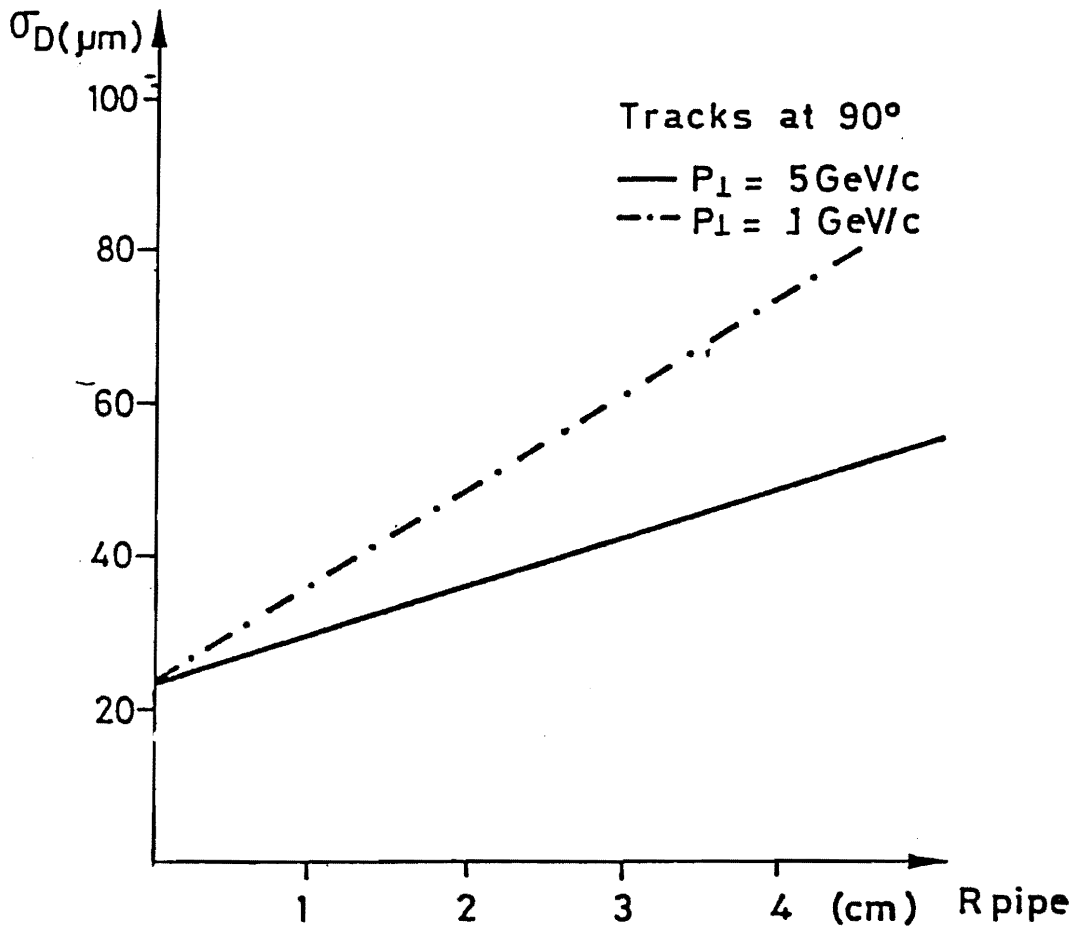


Fig. 7

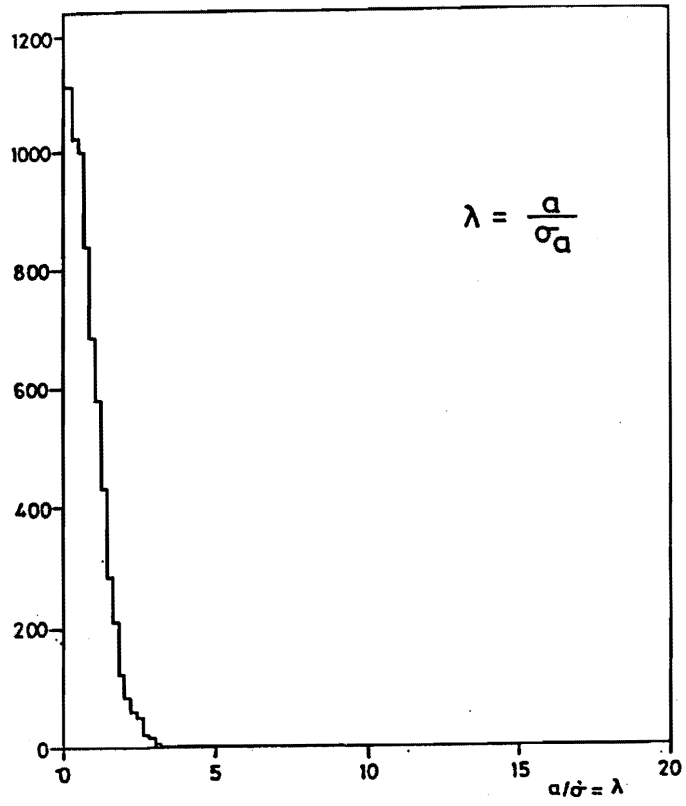


Fig. 8

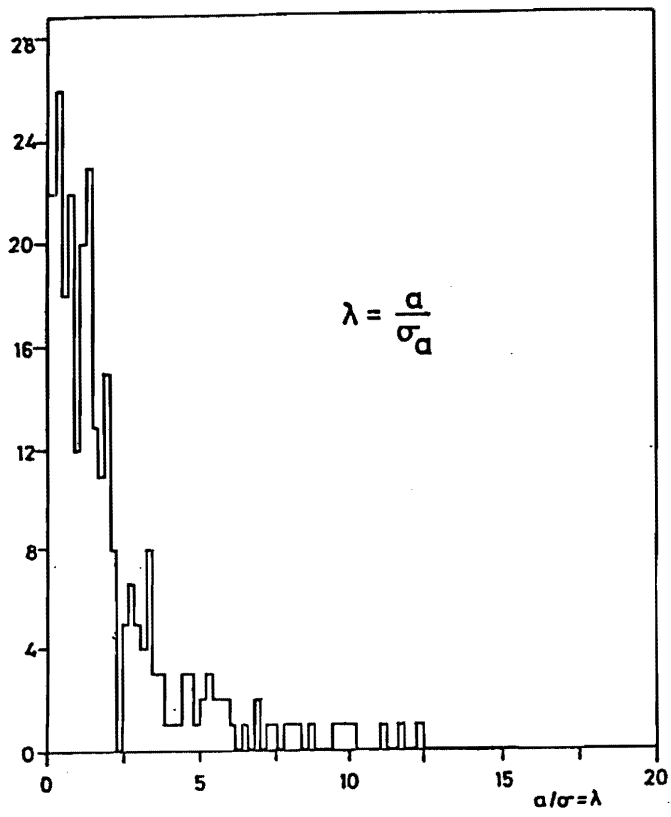


Fig. 9

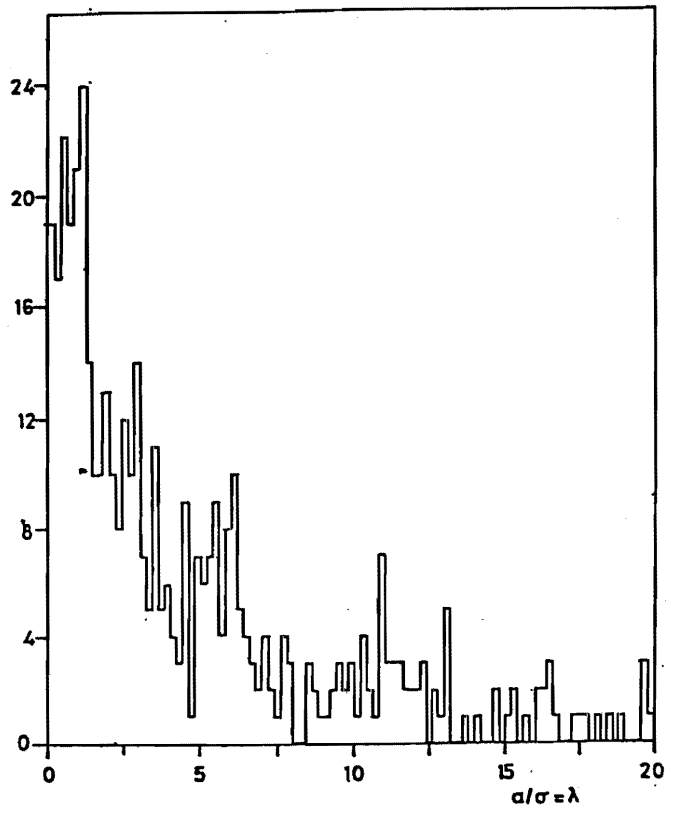


Fig. 10

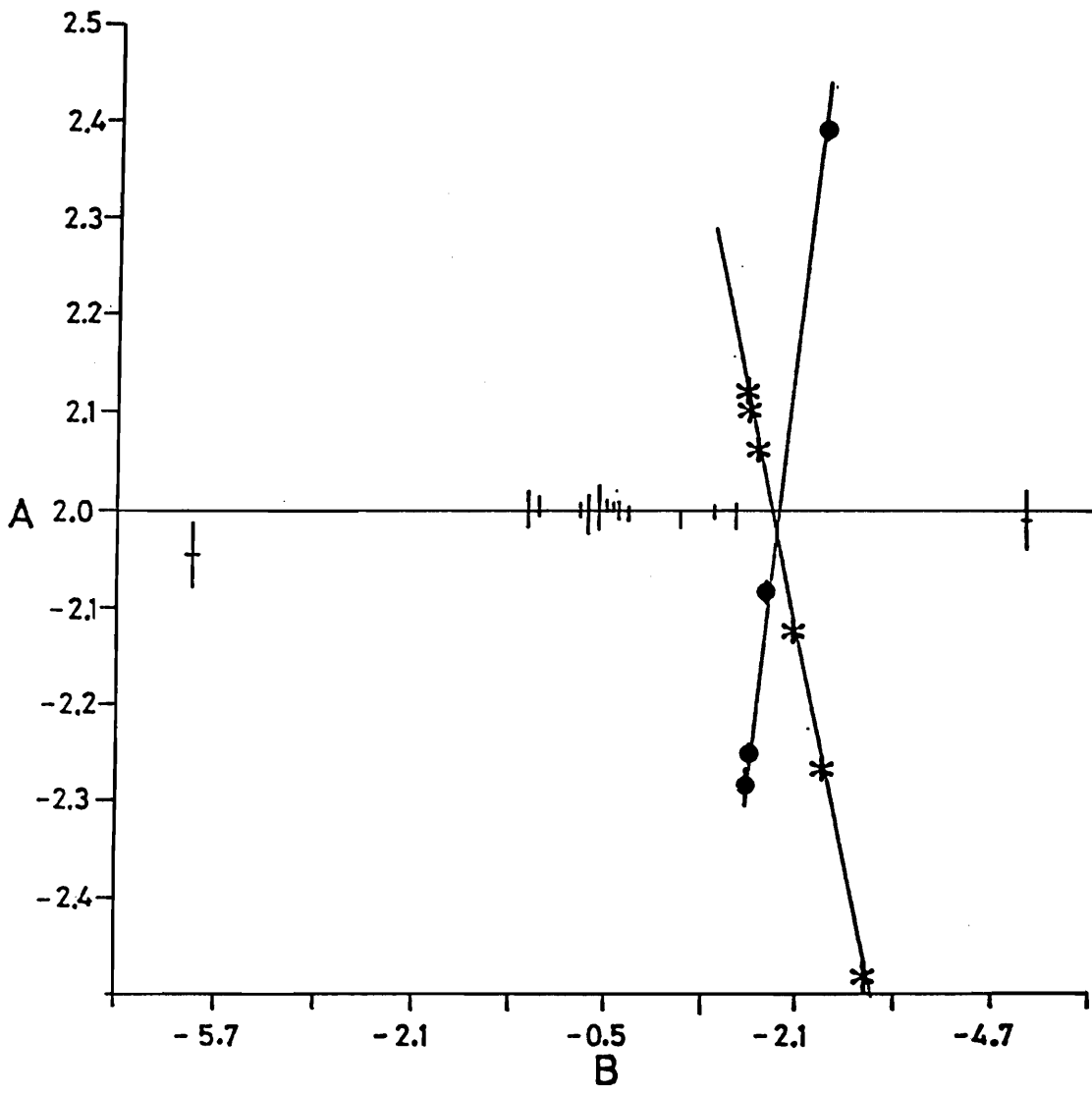


Fig. 11

$$\sqrt{S}=2000 \text{ GeV}, \int L dt = 10^{37} \text{ cm}^{-2}, b_{Tj} > 15 \text{ GeV}, |y| < 2$$

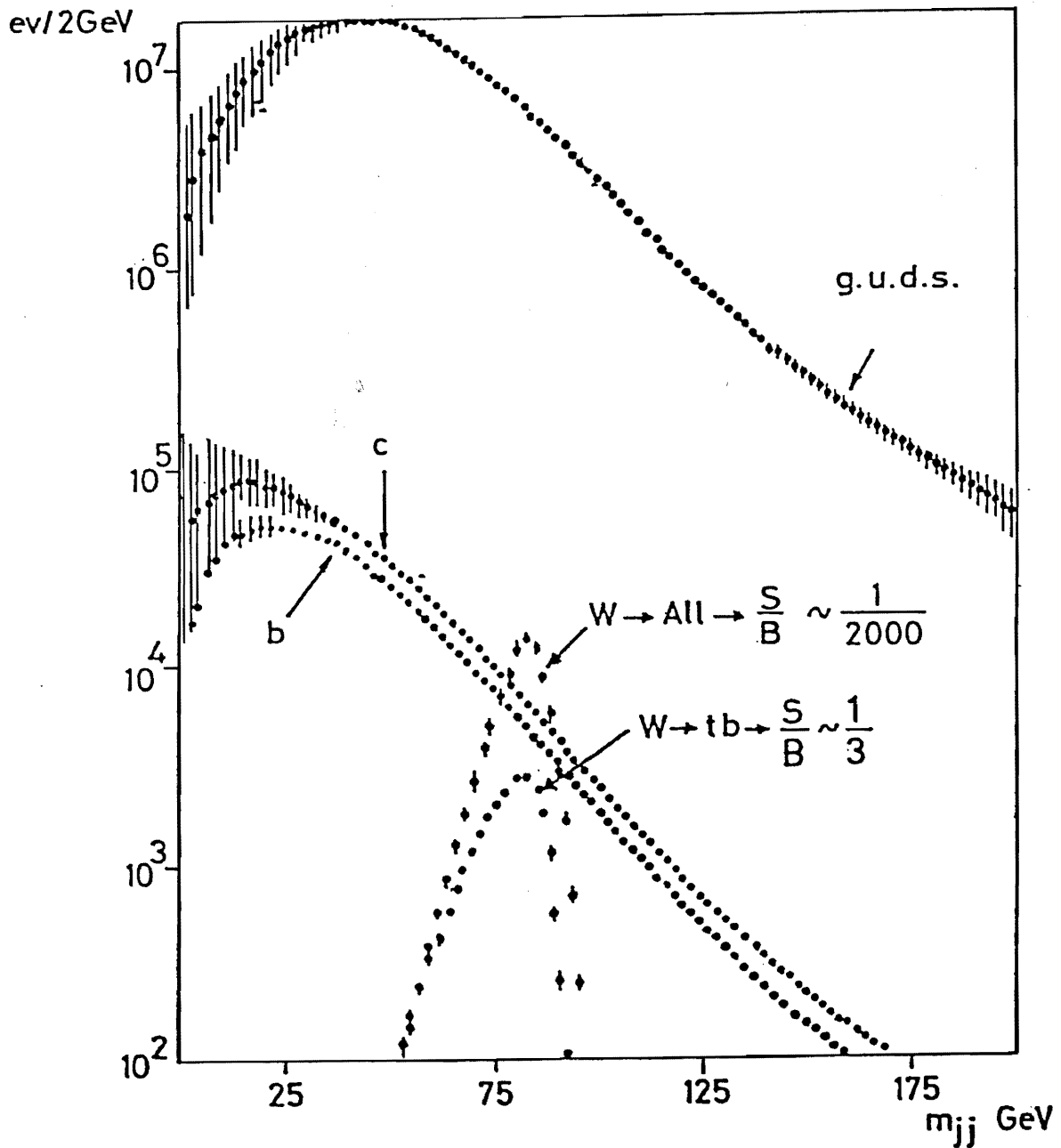


Fig. 12

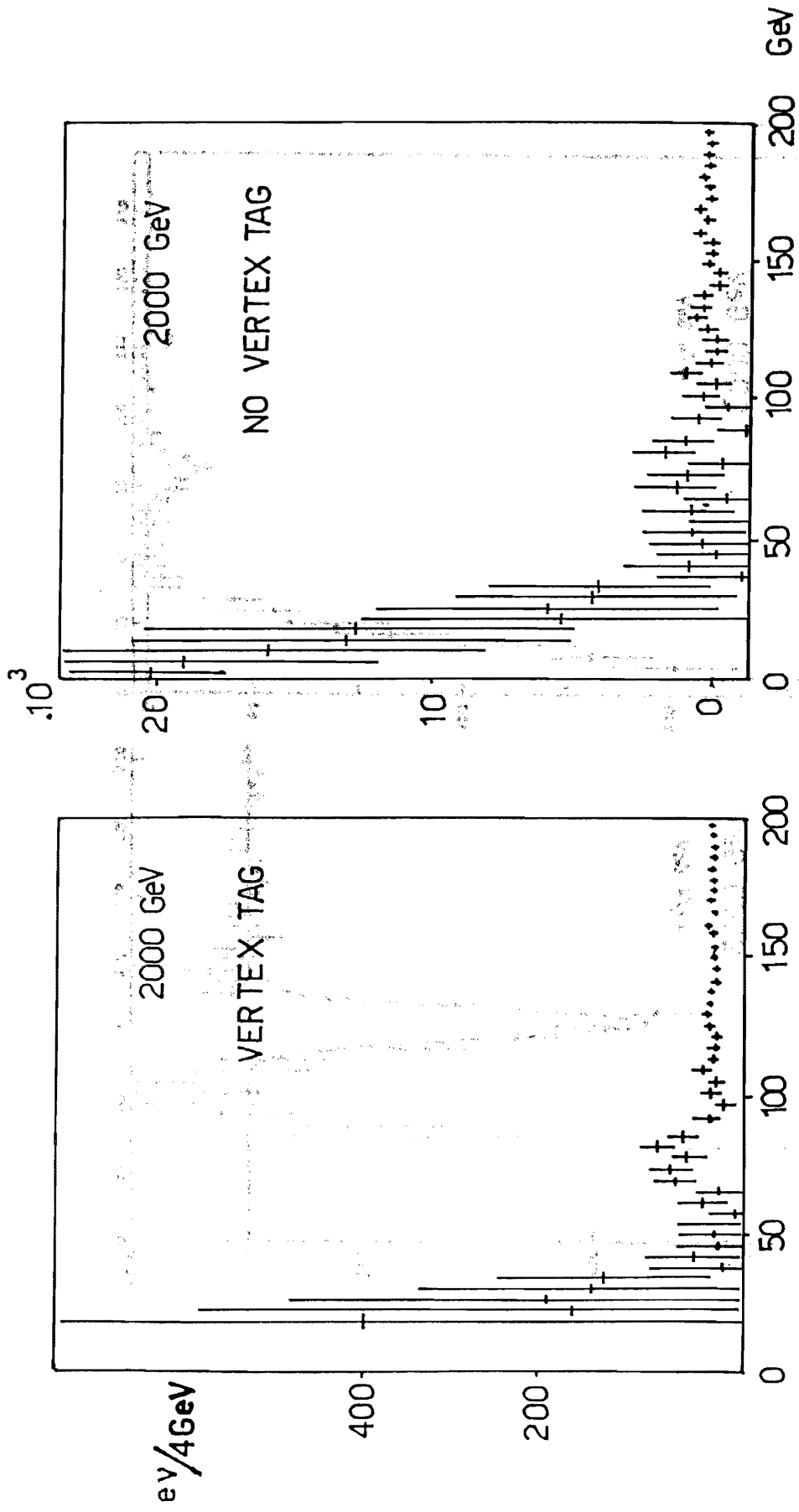


Fig. 13

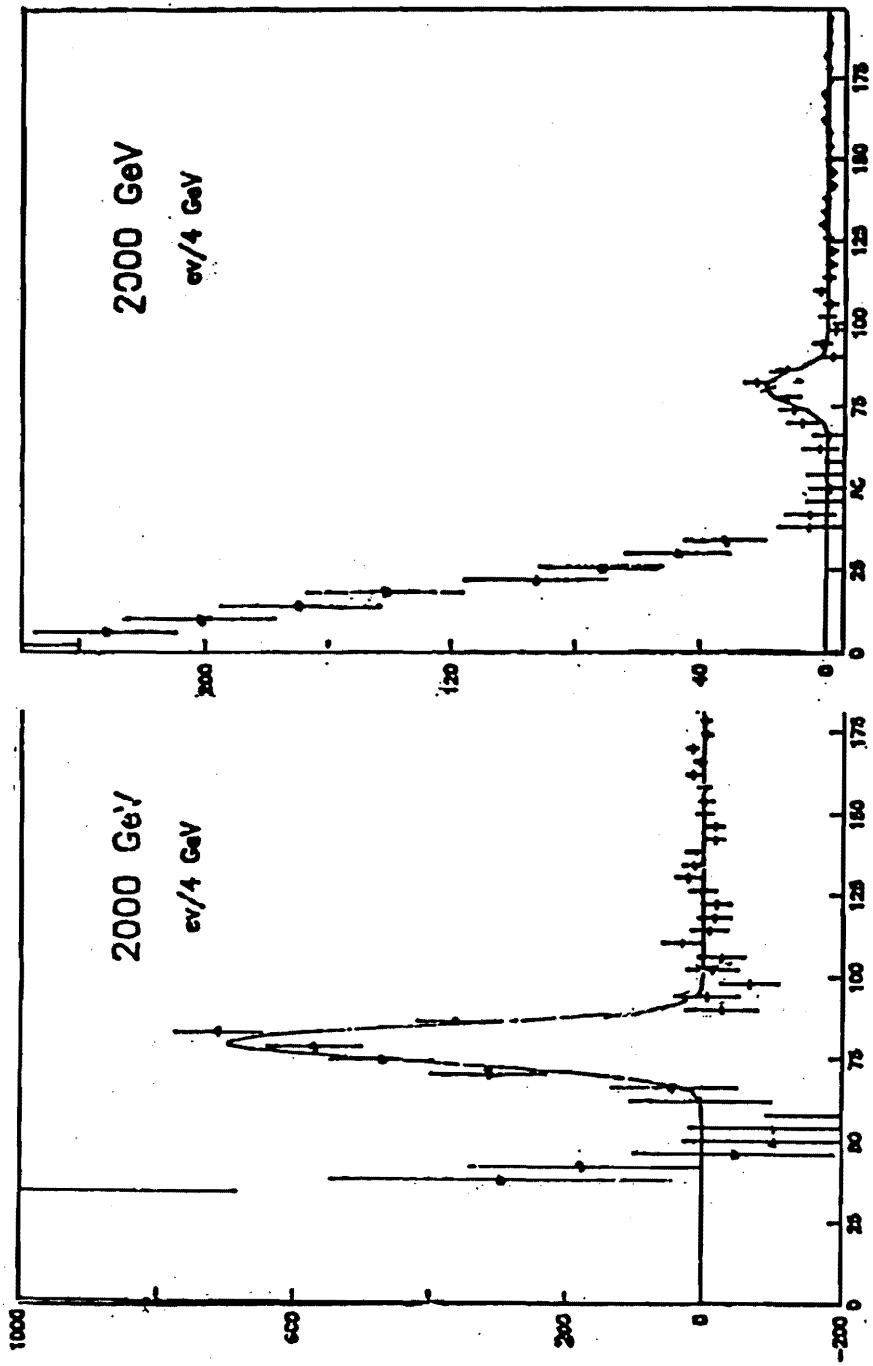


Fig. 14